Collider searches for the Higgs boson

Jared B. Stang

Abstract

In this report, we briefly review the role of the Higgs boson in electroweak symmetry breaking, before describing direct collider searches for this particle. We discuss experiments relevant to Higgs searches at LEP, the Tevatron, and the LHC.

1 Introduction

All of the particles in the Standard Model of Particle Physics, except one, have been observed, with the final missing quark, the top, being discovered at the Tevatron in 1995 [1, 2]. The elusive ingredient in the scheme is the Higgs boson. The Higgs plays an important role in the theory; it is responsible for electroweak symmetry breaking, a process that allows the bosons and fermions to have mass, which is necessary for agreement with observation. Confirming the existence of the Higgs would be a final triumph of the hugely successful Standard Model of Particle Physics. Alternatively, observing its absence will be hard evidence for physics beyond the Standard Model at electroweak scales (since the Higgs vacuum expectation value is at the electroweak scale). Due to the overwhelming success of the Standard Model, among other reasons, many expect the Higgs to be found soon: the high energy physics community is 'very pro-Higgs'[1].

We begin this note with a review of the Higgs mechanism of electroweak symmetry breaking in the Standard Model. Then, we discuss experimental efforts towards the discovery, or exclusion, of the Standard Model Higgs boson. We will focus on direct searches for the Higgs, of which the main players in the game include LEP (Large Electron-Positron Collider) at CERN, the Tevatron at Fermilab, and, now, the LHC (Large Hadron Collider) at CERN. We will identify the main channels in which these direct searches take place, and briefly discuss how these experiments come to their bounds. Using direct searches, LEP and the Tevatron have placed exclusion bounds on the mass of the Higgs, which, in addition to the data from precision electroweak experiments, puts the expected mass of the Higgs comfortably in the range of the LHC.

The current expectation for the mass of the Higgs boson is [3, 4, 5]:

$$114.4 \text{ GeV} < m_h < 158 \text{ GeV} \quad \text{or} \quad 173 \text{ GeV} < m_h < 193 \text{ GeV}. \tag{1}$$

LEP puts the lower bound of 114.4 GeV on the Higgs while the Tevatron results exclude the area $158 \text{ GeV} < m_h < 173 \text{ GeV}$. The upper bound is due to a global fit of the Standard Model to precision electroweak data, which will not be discussed here.

2 Review of Higgs phenomenology

In this section, we give a brief review of the Standard Model, with a focus on the role of the Higgs boson in symmetry breaking [6, 7]. As well, we figure out the coupling of the Higgs to the other Standard Model particles, for reference to later, before discussing the main branching ratios of importance in the direct searches we will review below.

2.1 The Standard Model

The first step in writing down the Standard Model is to identify the symmetry group under which fields will transform. This is

---

[1]Personal correspondence with David Morrissey.

$$G = SU(3)_c \times SU(2)_L \times U(1)_Y \ , \tag{2}$$

where fields possessing colour transform under the $SU(3)_c$ and the rest of the group makes up the electroweak sector. The corresponding spin-one gauge bosons are: 8 spin-one particles, G_μ^α, with the $SU(3)_c$; 3 spin-one W_μ^a's with the $SU(2)_L$, and; one gauge field B_μ corresponding to the hypercharge symmetry $U(1)_Y$. Having this, we now need to identify the field content of the theory. The fermion content of the Standard Model is given by three generations of the following representations under G:

$$Q_L = (\mathbf{3}, \mathbf{2}, 1/6) = \begin{pmatrix} u_L \\ d_L \end{pmatrix} \tag{3}$$

$$u_R = (\mathbf{3}, \mathbf{1}, 2/3) \tag{4}$$

$$d_R = (\mathbf{3}, \mathbf{1}, -1/3) \tag{5}$$

$$L_L = (\mathbf{1}, \mathbf{2}, -1/2) = \begin{pmatrix} \nu_L \\ e_L \end{pmatrix} \tag{6}$$

$$e_R = (\mathbf{1}, \mathbf{1}, -1) \ . \tag{7}$$

The second equality writes the non-trivial fields in $SU(2)_L$ space. Here, Q_L, u_R, and d_R make up the quarks, while L_L and e_R are the leptons; these are all fermions, or spin-1/2 particles, under Lorentz transformations. In the Standard Model, there is also a fundamental complex scalar field. This is the Higgs scalar, given by

$$\Phi = (\mathbf{1}, \mathbf{2}, 1/2) = \begin{pmatrix} \phi^+ \\ \phi^0 \end{pmatrix} \ . \tag{8}$$

Now, given this field content, we write down the Lagrangian:

$$\mathcal{L} = \mathcal{L}_{gauge} + \mathcal{L}_{Yukawa} + \mathcal{L}_{Higgs}. \tag{9}$$

$\mathcal{L}_{gauge}$ contains the gauge invariant kinetic terms for the gauge bosons and fermions, and is completely fixed by requiring gauge invariance. We will not need its form here. The Yukawa coupling term,

$$-\mathcal{L}_{Yukawa} = y_u \bar{Q}_L \tilde{\Phi} u_R + y_d \bar{Q} \Phi d_R + y_e \bar{L}_L \Phi e_R + (\text{h.c.}) \ , \tag{10}$$

where $\tilde{\Phi} = i\sigma^2 \Phi^*$, is the most general set of gauge invariant and renormalizable interactions that you can write down for these fields. We have suppressed generation indices in this expression, so that, for example, y_u is actually a matrix in generation space. Notice in particular that there are no mass terms for the fermion fields, as these are not invariant. At this stage then, the fermions are massless. We expect some mechanism to allow mass terms here; the general framework we are familiar with is the

Higgs mechanism of spontaneous symmetry breaking. The final piece of the puzzle, that accomplishes this, is the Higgs Lagrangian,

$$\mathcal{L}_{Higgs} = |D_m \Phi|^2 - V(|\Phi|) \tag{11}$$

$$= |(\partial_\mu + ig\frac{\sigma^a}{2}W_\mu^a + ig'\frac{1}{2}B_\mu)\Phi|^2 - (-\mu^2|\Phi|^2 + \frac{\lambda}{2}|\Phi|^4), \tag{12}$$

where we have introduced the weak and hypercharge couplings g and g'. The potential has been put in by hand to generate a symmetry breaking vacuum state; indeed, the minimum of the potential occurs for a non-zero vacuum expectation value of Φ:

$$\langle \Phi^\dagger \Phi \rangle = \frac{\mu^2}{\lambda} := v^2. \tag{13}$$

This allows us to expand Φ as (in a suitable choice of gauge)

$$\Phi(x) = \begin{pmatrix} 0 \\ v + \frac{h(x)}{\sqrt{2}} \end{pmatrix}, \tag{14}$$

where $h(x)$ is the Higgs boson. Recall that v can be determined from experiment; measuring the Fermi coupling G_F via precision electroweak measurements is enough to determine $v \approx 174$ GeV.

2.2 Higgs couplings

The non-zero vacuum expectation value (vev) of Φ brings with it some very important consequences. First, notice that upon putting Eq.(14) into Eq.(12), we generate mass terms for (certain combinations of) the gauge bosons W_μ^a and B_μ. Now, Φ, being a 2-component complex scalar, has four degrees of freedom, only one of which is included in Eq.(14). The other three degrees of freedom get 'eaten' by the previously massless gauge bosons to form the three massive gauge bosons of the Standard Model, $W^\pm$ and Z, leaving one massless gauge boson, the photon γ. In this manner, the vev of the Higgs field breaks the symmetry of the electroweak sector of G down to a $U(1)_{em}$, which we identify with the electromagnetic force. From Eq.(12), we also get the couplings of the Higgs to the gauge bosons ($V = W^\pm, Z$) and the couplings of the Higgs to itself [5]:

$$g_{hVV} = \frac{\sqrt{2}m_V^2}{v}, \quad g_{hhVV} = \frac{m_V^2}{v^2}, \quad g_{hhh} = \frac{3m_h^2}{\sqrt{2}v}, \quad g_{hhhh} = \frac{3m_h^2}{\sqrt{2}v^2}. \tag{15}$$

The vertex factor corresponding to these is given by the above coupling multiplied by i (and the metric tensor, $g^{\mu\nu}$, for those involving vector bosons).

The second important consequence of this symmetry breaking can be seen by inserting Eq.(14) into Eq.(10). After quark field generation rotations, we get diagonal terms like $\bar{u}'_L u'_R$, resulting in fermion masses that depend on the Yukawa coupling y_u and the Higgs vev v. Putting in a symmetry breaking potential for the Higgs then allows

the Standard Model fermions to gain mass, in accordance with observations. Furthermore, we get interactions between the Higgs and the fermions, which are concisely summarized, for a fermion f, as

$$g_{hf\bar{f}} = \frac{m_f}{\sqrt{2}v}. \tag{16}$$

2.3 Branching ratios of the Higgs

The branching ratios of the Higgs can be partially explained by appealing to the derived couplings, equations (15) and (16). Recall that each vertex adds a multiplicative factor of the corresponding coupling g_i to the amplitude; the branching ratio (is proportional to the decay rate, which in turn) is proportional to the squared amplitude. Thus, we can extract some of the expected behaviour of the branchings from the couplings. The Higgs vev is relatively large so that the couplings with v^2 in the denominator are suppressed relative to the same vertices with one less Higgs.

Now, notice that the coupling of the Higgs to a fermion f is proportional to m_f. Hence, we expect a larger branching ratio for decays to fermions with a larger mass. This can be seen in Figure 1: for small m_h, the dominant decay is $h \to b\bar{b}$, followed by $h \to \tau\bar{\tau}$ and $h \to c\bar{c}$. For small m_h, the decay to a $t\bar{t}$ pair is kinematically suppressed; the top quark is too heavy to be created on shell. For larger values of the Higgs mass, this decay plays an important role, as can be seen in Figure 2 for $m_h > 300$ GeV. The decay to gluons is mediated by a virtual $t\bar{t}$ pair; decay to a single gluon is forbidden by conservation of momentum, as is clear if we go to the Higgs rest frame.

The Higgs coupling to a vector boson V is proportional to m_V^2, so that we expect a large contribution from these decays for large enough Higgs masses that they are not kinematically suppressed. We can see this in Figures 1 and 2: for $m_h > \sim 140$ GeV, the decay $h \to W^+W^-$ dominates, followed shortly by the decay to neutral bosons $h \to ZZ$. Below the mass threshold ($m_h < 2V$), one of the vector bosons is virtual. These properties make the Higgs search at high masses relatively easy, as a signature, distinct from the QCD background, is expected when the vector bosons decay leptonically. This will be discussed further in the context of Tevatron and LHC searches, below.

3 Collider searches for the Higgs boson

In [9], Perelstein gives a general account of the process one undertakes to study the possibility of new particles within the range of a particular experiment[2]. First, one must study the possible production mechanisms for the particle, and compute the cross-sections, to ensure that the particle will be produced in observable amounts. Next, one has to consider all possible decay routes for the particle, and identify which of these may lead to a promising signal. This is to be done in conjunction with a determination of all the Standard Model background processes that may appear in

---

[2]Perelstein gives a 'twelve-step' process; I shorten this considerably.
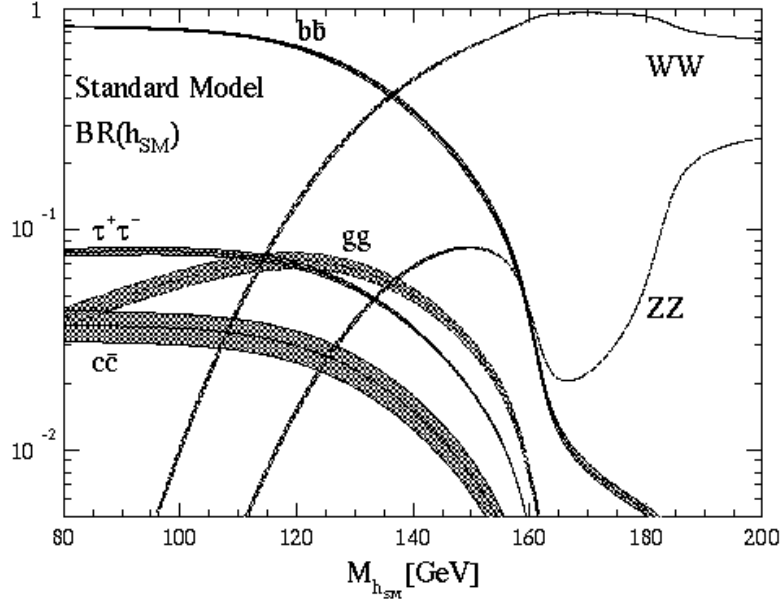
Figure 1: Branching ratios of the Standard Model Higgs at low m_h [8]. For values relevant to LEP searches, the decay to $b\bar{b}$ dominates.
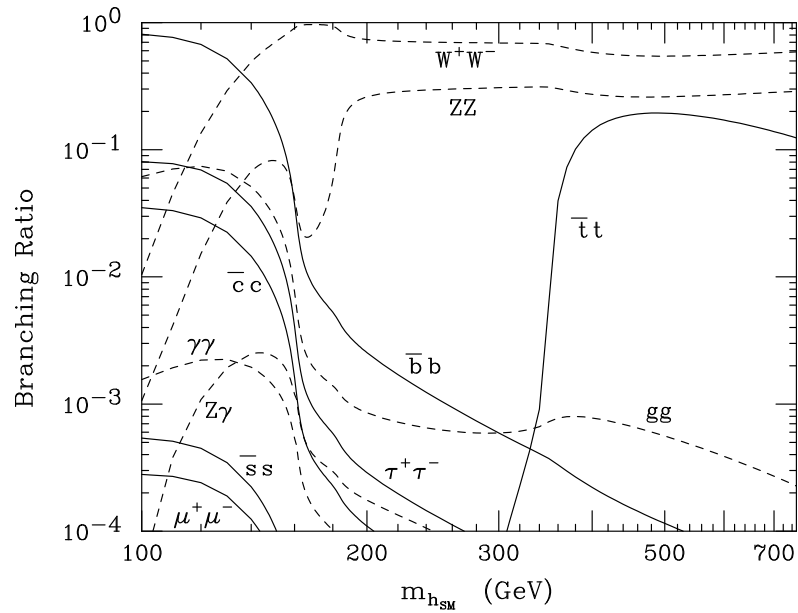
Figure 2: Branching ratios of the Standard Model Higgs at high m_h [5]. For large Higgs masses, vector boson decays dominate.
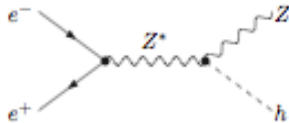
Figure 3: Higgsstrahlung production of the Higgs boson with a massive vector boson [9]. This is the primary production channel expected in the LEP studies.

the detector, and interfere with the signal. Finally, one arrives at the most promising channels for production and observation, given the experiment type and the energies accessible. It should be mentioned also that the luminosity of the collider is important here; a higher luminosity means more events, so that less prominent signals may be observed.

The main participants in the search for the Higgs in the past two decades have been LEP, the Tevatron, and, most recently, the LHC. We will discuss each of these colliders in turn, detailing the experimental efforts towards a direct observation of the Higgs boson. This will include an identification of the relevant production interactions and the most prominent search channels before a summary of the most recent results.

3.1 LEP

The LEP Collider at CERN, a positron-electron collider, was operational between 1989 and 2000. The centre-of-mass energy for this machine began around 90 GeV, suitable for studying the Z boson, while subsequent improvements and upgrades allowed LEP to explore collisions with $\sqrt{s}$ as high as 209 GeV by the end of its lifetime. Precision electroweak measurements had placed an upper bound on the Standard Model Higgs boson mass, but LEP was the first experiment to directly search for Higgs particles. Here, we report final results from the four LEP collaborations, ALEPH (Apparatus for LEP PHysics at CERN), DELPHI (DEtector with Lepton, Photon and Hadron Identification), L3, and OPAL (Omni-Purpose Apparatus for LEP), compiled after the machine completed operation. Prior to the results presented here, the four collaborations placed a lower bound of 107.9 GeV on the mass, at the 95% confidence level. We focus on the final year of LEP operation, in which a total of 2461 pb^{-1} of data at centre-of-mass energies between 189 and 209 GeV allowed the lower bound on the Higgs mass to be extended [3].

The main production of the Standard Model Higgs boson at LEP was expected to be via the Higgsstrahlung process, $e^+e^- \rightarrow hZ$, in which a produced Z boson radiates a Higgs (see Figure 3). At these energies, a small contribution is also expected from W and Z boson fusion, in which the Higgs is produced from two vector bosons radiated from the electron-positron beams; the final state here involves the Higgs and two neutrinos or an electron-positron pair. Recall that the mass of the Z boson is about 91 GeV; then, if produced with an on-shell Z, the mass range of the Higgs produced at

LEP would be between 100 and 120 GeV. At these energies, the main decay process is into $b\bar{b}$ (with a branching ratio of $\sim74\%$ for a Higgs mass of 115 GeV), with secondary decays to $\tau^+\tau^-$, WW, gg ($\sim7\%$ each), and $c\bar{c}$ ($\sim4\%$), as can be seen in Figure 1.

Recall that in collider experiments, quarks appear as QCD jets, neutrinos are not detected, and leptons can be identified. Possible final state topologies searched for here were the four-jet final state ($h \to b\bar{b}$, $Z \to q\bar{q}$), the missing energy final state ($h \to b\bar{b}$, $Z \to \nu\bar{\nu}$), the leptonic final state ($h \to b\bar{b}$, $Z \to l^+l^-$), where l is an electron or a muon, and the tau lepton final states ($h \to b\bar{b}$, $Z \to \tau^+\tau^-$) and ($h \to \tau^+\tau^-$, $Z \to q\bar{q}$). Many cuts are applied to the data to reduce the background; b-tagging of the Higgs decay products plays an important role here, as does the identification of leptons and missing transverse energy.

For each possible outcome, each experiment reports the number of observed data events in addition to the number of expected events, both for background only and for signal plus background. These estimates are given by Monte Carlo simulations based on detailed information about the experimental event, including centre-of-mass energy, integrated luminosity, selection efficiencies, and experimental resolutions. With these in hand, they study the log-likelihood ratio

$$LLR = -2\ln\frac{p(\text{data}|H_{s+b})}{p(\text{data}|H_b)}, \qquad (17)$$

where $p(\text{data}|H_b)$ ($p(\text{data}|H_{s+b})$) is the probability, or likelihood, of the background (signal plus background) hypothesis, given some data set. If it is more likely that the data fits the signal plus background hypothesis, then $LLR < 0$, while if the background-only hypothesis is more likely, $LLR > 0$. Using LLR as the test statistic also has the advantages that it is related to the difference in χ^2 between both hypotheses and that it can be written as a sum of contributions from individual events, allowing one to easily study results in different channels.

For the combined data from the four LEP experiments, the plot showing the expected and observed behaviour of the test statistic LLR is shown in Figure 4. As can be seen in the figure, the LEP experiment discriminates well between the background hypothesis and the signal plus background hypothesis for lower values of the Higgs mass, as the median value of the background and the signal plus background distributions are well separated. The significance of the deviation of the observed LLR from the expected background can be quantized by the plotted 1- and 2-σ bands. Observations in this range were consistent with the background hypothesis, leading to a final result, at the 95% confidence level, of

$$m_h > 114.4 \text{ GeV} \quad \text{(LEP result)}. \qquad (18)$$

3.2   Tevatron

The Tevatron at Fermilab, in Illinois, was completed in 1983, and will collide $p\bar{p}$ beams at centre-of-mass energies up to 1.96 TeV until September 2011. Before the LHC, the
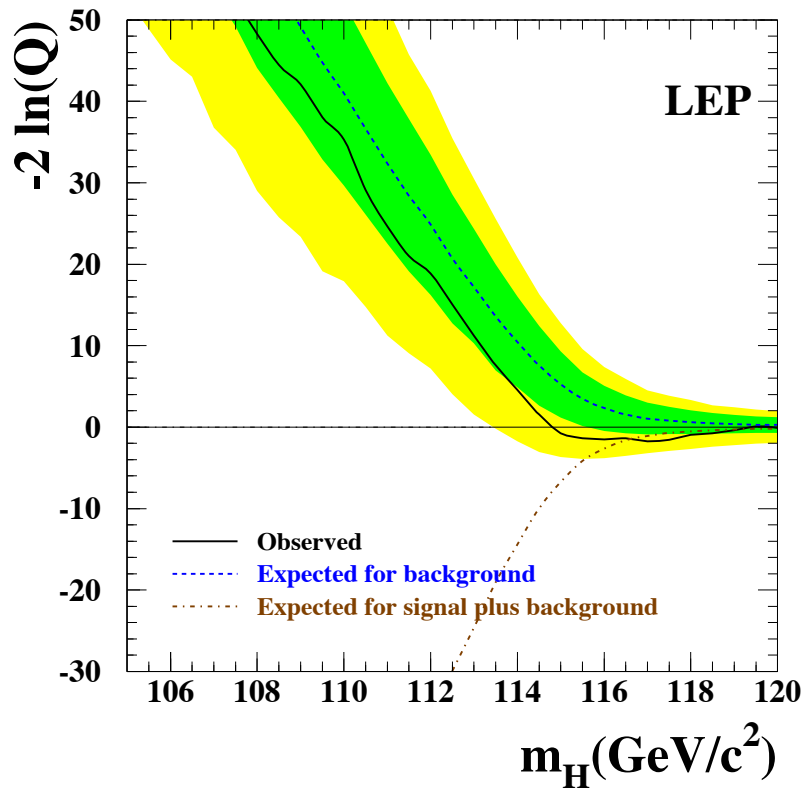
Figure 4: Observed and expected behaviour of the log-likelihood ratio $LLR = -2\ln Q$ at LEP [3]. The expected value for the background is shown with 1- and 2-σ bands around the median. Note the large discriminatory power for small Higgs masses, as can be seen by the large difference in the 'Expected for background' and the 'Expected for signal plus background' curves.
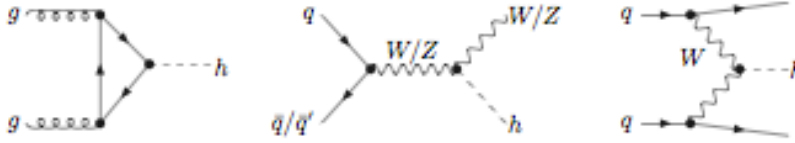
Figure 5: Higgs production channels at the Tevatron [9]. These are, from left to right, gluon-gluon fusion, production with a vector boson, and vector boson fusion. Gluon-gluon fusion has the largest cross-section at the Tevatron (see Figure 6).

Tevatron was the highest energy particle collider in the world, and enjoyed a scientifically successful lifetime that included the discovery of the top quark. Now, funding has been reduced, and the Tevatron is set to shut down later this year. The two main detectors, CDF (Collider Detector at Fermilab), and D0, have performed direct searches for the Standard Model Higgs boson at the energies available. We describe the latest results from these experiments, which, using up to 8.2 fb^{-1} of data, slightly extends the excluded region [4].

The main channel for Higgs production at the Tevatron is gluon-gluon fusion ($gg \to h$), due to the large luminosity of the gluon partons in high energy colliders. This process involves gluon partons from the incident $p\bar{p}$ pair and is mediated by a fermion loop, like the gluon-gluon decay $h \to gg$. Secondary channels include production with a vector boson ($q\bar{q} \to Vh$), and vector boson fusion ($q\bar{q} \to q'\bar{q}'h$) (See Figure 5 for the diagrams associated with these processes, and Figure 6 for the Higgs production cross-section at Tevatron). As can be seen in Figure 1, at the Higgs mass values studied here ($155 < m_h < 180$ GeV), the dominant branching ratio is to W^+W^-. The study described here focusses on this vector boson decay mode $h \to W^+W^-$, and includes some acceptance for decays to $\tau^+\tau^-$ and $\gamma\gamma$. Here, CDF and D0 can search for events in which both W bosons decay leptonically, characterized by missing transverse momentum and two oppositely-charged and independent leptons. Events can be catagorized according to which leptons are present in the decay, and the number of jets in the event. The experiments consider many possibilities here, in addition to the $\tau^+\tau^-$ and $\gamma\gamma$ decays, resulting in 46 mutually exclusive final states that can be identified.

The analysis done on the data from Tevatron was more involved than that performed for LEP; to ensure that the final result does not depend on the statistical framework, the experiments combine all the search channels using both the Bayesian and the Modified Frequentist methods (LEP used only the Modified Frequentist method). A plot of the log-likelihood ratio, including the median value for the signal plus background hypothesis and the distribution for the background-only hypothesis, is shown in Figure 7. As in the LEP results, we see a large discriminatory power in a subset of the range; here, it is in the middle of the plot. These most recent results from Tevatron exclude, at the 95% confidence level, the region

$$158 < m_h < 173 \text{ GeV} \quad \text{(Tevatron excluded).} \quad (19)$$

9
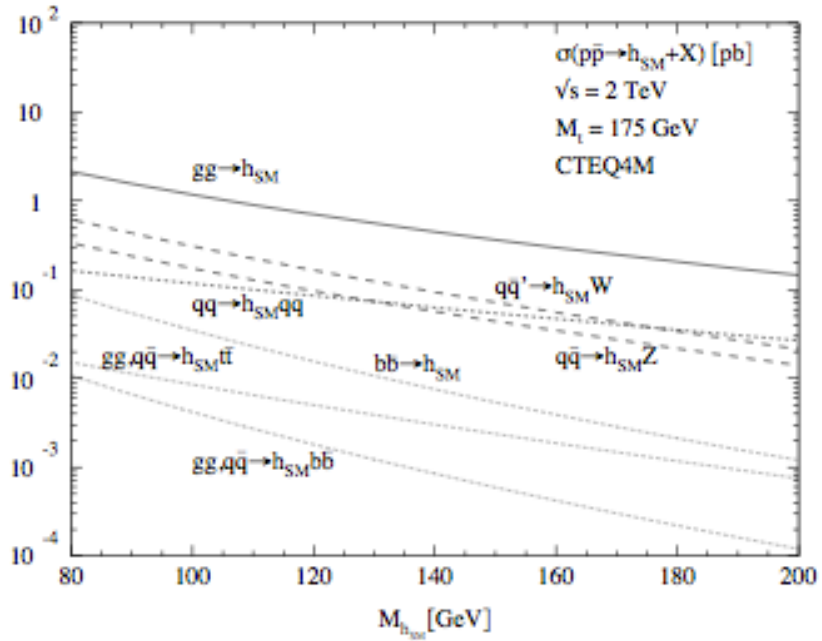
Figure 6: Cross-sections for Higgs production at $\sqrt{s} = 2$ TeV, centre-of-mass energy relevant for the Tevatron [5, 8]. Gluon-gluon fusion has the largest cross-section, followed by Higgs production with a vector boson and vector boson fusion.
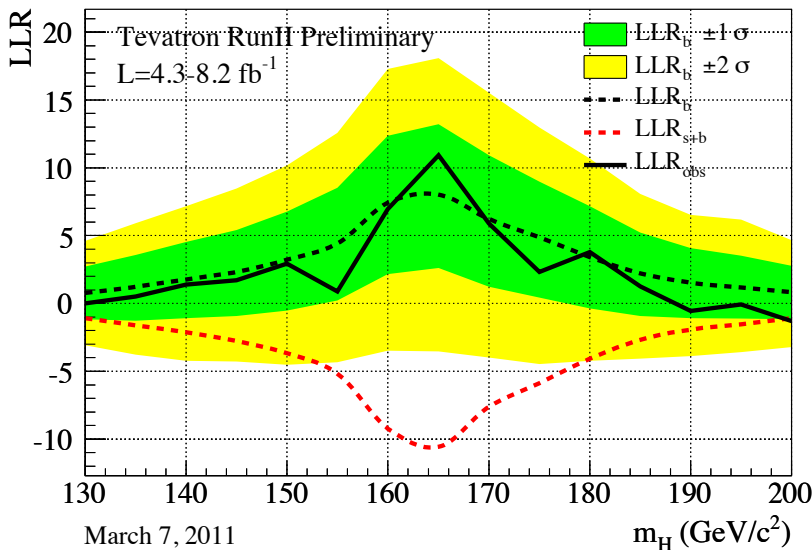
Figure 7: Observed and expected behaviour of the log-likelihood ratio at the Tevatron [4]. The expected value for the background is shown with 1- and 2-σ bands around the median. Here, we see a a large discrimination for values of the Higgs mass in the middle of the plot.

3.3 LHC

The LHC at CERN, a *pp* collider, replaced the LEP Collider in the 27 km circumference tunnel below Switzerland and France. The idea of the LHC started in the early 1980's, although it was not until 1994 that CERN approved its construction. In late 2009, the LHC circulated its first beam, at an energy of 0.9 TeV. A later increase in energy to 2.36 TeV broke the world record, surpassing the Tevatron and making the LHC the highest energy particle collider on the planet. In March 2010, the collider ramped up its energy to $\sqrt{s} = 7$ TeV, at which it has been operating for the past year, save for a winter maintenance shutdown. In 2013, a longer shutdown is planned to prepare for the final increase in energy to the maximum value of $\sqrt{s} = 14$ TeV.

3.3.1 CMS preliminary results

The CMS (Compact Muon Solenoid) experiment at the LHC has recently released results of direct searches for the Higgs boson with 36 pb^{-1} of data at centre-of-mass energies of 7 TeV, which we review here [10]. In this report, CMS sought the Higgs in the mass range $120 < m_h < 600$ GeV, looking for the Standard Model Higgs boson.

Higgs production at the LHC is expected to be enhanced as compared to the Tevatron, although the main processes of gluon-gluon fusion and vector boson fusion still give the largest contribution to the cross-section (recall Figure 6). This study searches for the Higgs in the mass range $120 < m_h < 600$ GeV; referring to Figure 2, across this

range, the dominant branching ratio is the decay to W^+W^-. Accordingly, they search for the Higgs only in the $h \to W^+W^-$ decay mode.

To identify Higgs events (that decay in this way) the experiment first has to identify W^+W^- events. As mentioned above, for the Tevatron, this is simplest when both W bosons decay leptonically. The main identifier of these leptonic events is the existence of two oppositely charged leptons with high transverse momentum, in one of three final states: e^+e^-, $\mu^+\mu^-$, or $e^{\pm}\mu^{\mp}$ (these include the possible $W \to \tau\nu$ events in which the τ decays leptonically). There are many cuts that can narrow the data set; we describe three of them. First, the charged lepton decay products are expected to be isolated from the rest of the event; this is assured by making a cut on any lepton with too much activity in a cone around its trajectory. Next, recall that neutrinos do not show up in the detectors, resulting in missing transverse energy. A cut is made on events that have missing energy below some threshold, to suppress the Drell-Yan background (the Drell-Yan process produces a lepton pair, without neutrinos, through an s-channel γ or Z.). Lastly, to further reduce the Drell-Yan background in the e^+e^- and $\mu^+\mu^-$ states, a Z veto, that rejects events with a dilepton invariant mass near the Z mass, is applied.

Now, to pick out possible Higgs decays from these W^+W^- events, they use two methods. The first makes a cut based on the angle between the final state leptons; leptons coming from a Higgs decay tend to have a small opening angle, while those from background events tend to emerge back-to-back. The second method uses correlations among the variables to determine if they are consistent with a Higgs event. For the data analyzed in [10], no deviation from the Standard Model background was found.

3.3.2 Future LHC prospects

As discussed in [5], with enough integrated luminosity, the Tevatron should be able to exclude, give evidence for (3σ evidence), or discover the Higgs (5σ discovery). However, even with a discovery, the Tevatron is too limited in scope and energy to study the properties of the Higgs, such as its couplings to vector bosons. On the other hand, Higgs production rates are much larger at the LHC. Within the first few years of operation, the LHC should be able to study the entire interesting Higgs mass range of the Standard Model, up to ~ 1 TeV, with enough data for a 5σ discovery. Further, the LHC will be able to effectively study any Higgs boson in this range, accurately determining its mass and couplings. As Carena says [5], 'there is no escape route for the SM Higgs boson at the LHC'.

4   Summary

The final particle that we expect to observe in the context of the Standard Model is the Higgs boson. Given the model's previous success, much experimental effort is being put towards the discovery of the Higgs.

Above, we reviewed results from the three main accelerators that have participated

in direct searches for the Higgs boson, in the past, present, and future. LEP, the electron-positron collider at CERN, placed a lower bound on the mass of the Higgs, before ceasing operation to make way for the LHC. The Tevatron excluded an interval of Higgs mass in the middle of what is believed to the be the possible range, and continues to run today, pushing to record more data before its eventual shut down later this year. In the near future, the LHC will take over, and, before long, will search the entire expected Higgs mass range of the Standard Model. It is expected that the LHC will allow the first glimpses into much anticipated physics beyond the Standard Model.

References

[1] CDF Collaboration, F. Abe *et al.*, Phys. Rev. Lett. **74**, 2626 (1995).

[2] D0 Collaboration, S. Abachi *et al.*, Phys. Rev. Lett. **74**, 2632 (1995).

[3] LEP Working Group for Higgs boson searches, R. Barate *et al.*, Phys. Lett. **B565**, 61 (2003), hep-ex/0306033.

[4] CDF and D0, T. Aaltonen *et al.*, (2011), 1103.3233.

[5] M. S. Carena and H. E. Haber, Prog. Part. Nucl. Phys. **50**, 63 (2003), hep-ph/0208209.

[6] C. Burgess and G. Moore, *The standard model: A primer* (Cambridge University Press, Cambridge, UK, 2007).

[7] D. Morrissey, Phys 528 lecture notes, 2011.

[8] M. Spira, (1998), hep-ph/9810289.

[9] M. Perelstein, (2010), 1002.0274.

[10] CMS, S. Chatrchyan *et al.*, (2011), 1102.5429.